Electronic Journal of Mathematical Analysis and Applications
Vol. 13(1) Jan. 2025, No.15.
ISSN: 2090-729X (online)
ISSN: 3009-6731(print)
http://ejmaa.journals.ekb.eg/

STUDY OF THE DYNAMICS OF HIV-CHOLERA CO-INFECTION IN A MATHEMATICAL MODEL

A. S. ABDRAMANE, H. DJIMRAMADJI, M. S. DAOUSSA HAGGAR

Abstract. In this article, we propose and analyze a compartmental model for HIV-Cholera co-infection. We establish the existence, uniqueness, and positivity of the solution. The disease-free equilibrium (DFE) point is then identified and its local and global stability is analyzed to better understand the dynamics of this co-infection. A sensitivity analysis is conducted to explore potential strategies for limiting secondary infections. Finally, numerical simulations illustrate our theoretical results, showing that when the contact rate between susceptible and infected individuals is significantly reduced, the infected population will decline, with cholera disappearing after 400 days and HIV after 500 days. This study highlights that the most influential parameters for controlling the disease are the contact rates β_H, β_C, and β_{HC}. Numerical results show that both diseases will disappear when the basic reproduction number $\mathcal{R}_0$ remains below one, but the diseases remain endemic in the population when $\mathcal{R}_0$ is greater than one.

1. Introduction

HIV/AIDS is a sexually transmitted disease that can also spread through contact with contaminated objects. The infection is caused by a retrovirus that transcribes its RNA into viral DNA after infecting a host cell, a process mediated by the enzyme reverse transcriptase [13].

The HIV virus contains three retroviral genes coding for various viral proteins. As of 2023, over 40 million people worldwide are living with HIV. The first mathematical model addressing HIV was introduced in 1986 [3].

A study by [5] described the seroprevalence of HIV among tuberculosis patients in Chad, analyzing epidemiological characteristics and associated risk factors. Additionally, [15] investigated the feasibility of cervical smear tests for HIV-positive women in Chad. Cervical cancer, a leading cause of cancer-related deaths among women in sub-Saharan

2020 *Mathematics Subject Classification.* 34A34, 34D20.
Key words and phrases. HIV, Cholera, Mathematical Modeling, Reproduction Number, Stability, Numerical Simulation.
Submitted Dec. 08, 2024.Revised Jan. 5, 2025. Accept Mar. 02, 2025.

Africa, has seen increased incidence due to HIV infection, reinforcing WHO recommendations for screening precancerous lesions[15]. While antiretrovirals have improved the survival of people living with HIV (PLHIV), emerging non-HIV-related comorbidities pose significant challenges for patient management [11].

Cholera, on the other hand, is an intestinal disease caused by the bacterium Vibrio cholerae, which colonizes the human gut. This pathogen is part of the environmental microbial community [6]. Standard bacteriological procedures to isolate V. cholerae from environmental samples, including water, are often unsuccessful between outbreaks [6]. Cholera transmission primarily occurs through contaminated water, food, and seafood from endemic regions [9]. The disease manifests as severe, profuse diarrhea, leading to acute dehydration and potentially death without prompt treatment [8]. Clinical forms include dry cholera, characterized by shock and rapid death; classic cholera, with diarrhea and vomiting, which can lead to fatal outcomes; and mild cholera, which may present no symptoms, requiring laboratory diagnosis. Treatment involves rehydration and antibiotics, while prevention includes sanitation measures, water treatment, and improved hygiene and nutrition [10].

Both cholera and HIV rank among the most significant infections in sub-Saharan Africa in terms of morbidity and mortality [4]. The impact of cholera on HIV represents a critical public health issue due to the complex interactions between the two infections and their consequences on population health. The WHO has issued recommendations on the use of antiretrovirals for HIV treatment since 2002, with subsequent revisions in 2003, 2006, and 2010 [13].

In this context, it is crucial to study the mutual effects of these two diseases on the spread of infection.

The objective of our study is to examine the impact of cholera on people living with HIV (PLHIV) in terms of transmission and recovery, and to analyze the dynamics of this co-infection using an SIR-type mathematical model. This model will provide a better understanding of the interactions between these two diseases.

2. Model formulation

We consider an epidemiological model of the SIR type to describe the dynamics of HIV and cholera propagation. Each population is subdivided into several subpopulations: S_H represents individuals susceptible to HIV, S_C represents individuals susceptible to cholera, S_{HC} represents individuals susceptible to both diseases, I_H represents individuals infected with HIV, I_C represents individuals infected with cholera, I_{HC} represents individuals co-infected with HIV and cholera, R_H represents individuals recovered from HIV, R_C represents individuals recovered from cholera, and R_{HC} represents individuals recovered from both diseases.

We assume that individuals recovered from HIV are those who have undergone antiretroviral (ARV) treatment. Additionally, the recruitment of susceptible individuals is constant and is denoted respectively by Λ_H for those susceptible to HIV, Λ_{HC} for those susceptible to both diseases, and Λ_C for those susceptible to cholera.

The transmission rates are given by:

- β_H, representing the rate at which individuals susceptible to HIV become infected,
- β_C, representing the rate at which individuals susceptible to cholera become infected,
- β_{HC}, representing the rate of simultaneous infection by both HIV and cholera.

Individuals infected with HIV and/or cholera die at rates μ_H for HIV and μ_C for cholera, respectively.

The interactions between co-infected individuals and susceptibles are modeled by the following terms:

- $\alpha_H I_{HC}$ represents contact between a co-infected individual and an individual susceptible to HIV,
- $\alpha_C I_{HC}$ represents contact between a co-infected individual and an individual susceptible to cholera.

Finally, γ_H and γ_C denote the recovery rates for HIV and cholera, respectively.

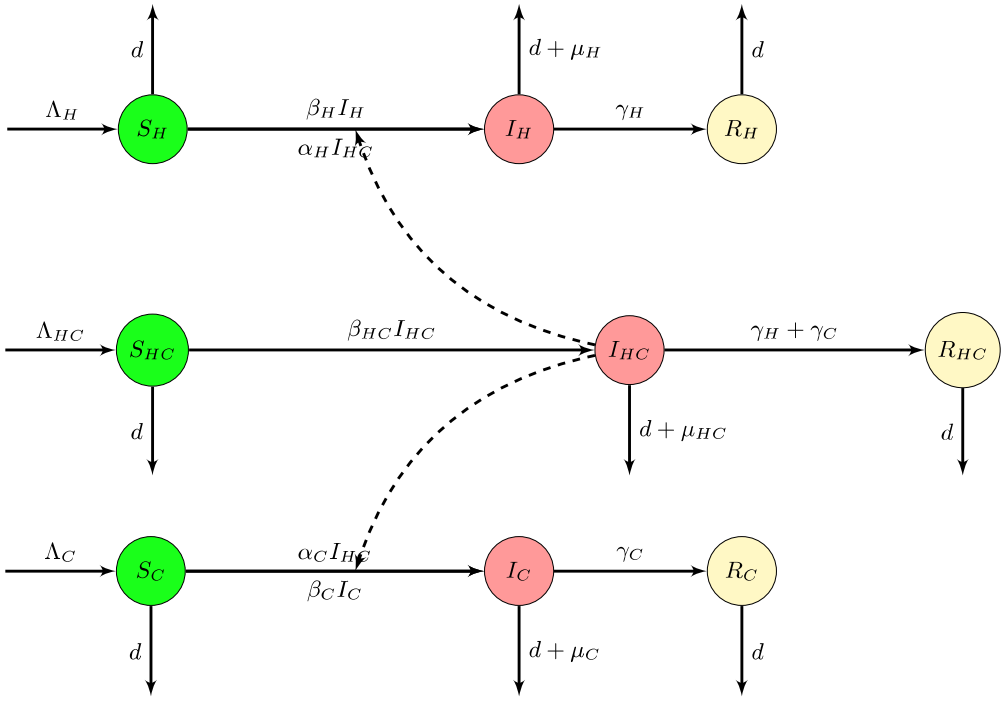

FIGURE 1. flot diagram

$$\frac{dS_H}{dt} = \Lambda_H - \beta_H S_H I_H - \alpha_H S_H I_{HC} - dS_H \tag{1a}$$
$$\frac{dS_C}{dt} = \Lambda_C - \beta_C S_C I_C - \alpha_C S_C I_{HC} - dS_C \tag{1b}$$
$$\frac{dS_{HC}}{dt} = \Lambda_{HC} - \beta_{HC} S_{HC} I_{HC} - dS_{HC} \tag{1c}$$
$$\frac{dI_H}{dt} = \beta_H S_H I_H - \gamma_H I_H + \alpha_H S_H I_{HC} - (d+\mu_H) I_H \tag{1d}$$
$$\frac{dI_C}{dt} = \beta_C S_C I_C - \gamma_C I_C + \alpha_C S_C I_{HC} - (d+\mu_C) I_C \tag{1e}$$
$$\frac{dI_{HC}}{dt} = \beta_{HC} S_{HC} I_{HC} - (\gamma_H + \gamma_C) I_{HC} - (d+\mu_{HC}) I_{HC} \tag{1f}$$
$$\frac{dR_H}{dt} = \gamma_H I_H - dR_H \tag{1g}$$
$$\frac{dR_C}{dt} = \gamma_C I_C - dR_C \tag{1h}$$
$$\frac{dR_{HC}}{dt} = (\gamma_H + \gamma_C) I_{HC} - dR_{HC} \tag{1i}$$

Equipped with initial conditions:

$$S_H(0) \geq 0, S_C(0) \geq 0, S_{HC}(0) \geq 0, I_H(0) \geq 0, I_C(0) \geq 0, I_{HC}(0) \geq 0, R_H(0) \geq 0, R_C(0) \geq 0, R_{HC}(0) \geq 0. \tag{1j}$$

Variable	Description
S_H	Density of the population healthy and not infected with HIV
I_H	Density of the population infected with HIV
R_H	Density of the population recovered from HIV
S_C	Density of the population healthy and not infected with cholera
I_C	Density of the population infected with cholera
R_C	Density of the population recovered from cholera
S_{HC}	Density of the population healthy and not infected with HIV/cholera
I_{HC}	Density of the population infected with both HIV and cholera
R_{HC}	Density of the population recovered from both HIV and cholera

TABLE 1. Table of model variables.

Parameters	Epidemiological Interpretation
Λ_H	Constant recruitment of population susceptible to HIV
Λ_C	Constant recruitment of population susceptible to cholera
Λ_{HC}	Constant recruitment of population susceptible to both diseases
β_H	HIV transmission rate
β_C	Cholera transmission rate
μ_H	Mortality rate due to HIV
μ_C	Mortality rate due to cholera
γ_H	Recovery rate from HIV
γ_C	Recovery rate from cholera
α_H	Effect of HIV on cholera transmission
α_C	Effect of cholera on HIV transmission

TABLE 2. Table of model parameters.

3. Mathematical analysis of the model

3.1. **Positivity.**

Theorem 1. *The components $S_H(t), S_C(t), I_H(t), I_C(t), R_H(t), R_C(t), I_{HC}(t), R_{HC}(t)$ remain positive for all time t.*

Proof. The equation (1a) implies

$$\frac{dS_H}{dt} = \Lambda_H - (\beta_H I_H + \alpha_H I_C + d)S_H,$$

which can be rewritten as:

$$\frac{dS_H}{dt} + f(t)S_H = \Lambda_H, \tag{2}$$

where $f(t) = \beta_H I_H(t) + \alpha_H I_C(t) + d$.

The solution to this differential equation is:

$$S_H(t) = e^{-\int_0^t f(\tau)d\tau}\left[S_H(0) + \Lambda_H \int_0^t e^{\int_0^s f(\tau)d\tau} ds\right] \geq 0.$$

Similarly, $S_C \geq 0$.

For I_{HC}, the equation (1f) implies:

$$\frac{dI_{HC}}{dt} = (\beta_{HC} S_{HC} - \gamma_H - \gamma_C - d - \mu_H - \mu_C) I_{HC},$$

whose solution is:

$$I_{HC}(t) = K e^{\int_0^t (\beta_{HC} S_{HC}(\tau) - \gamma_H - \gamma_C - d - \mu_H - \mu_C) d\tau} \geq 0.$$

Similarly, $I_C \geq 0$.

For I_H, the equation (1d) yields:

$$I_H(t) = e^{-\int_0^t g(\tau) d\tau} \left[I_H(0) + \alpha_H \int_0^t S_H(\tau) I_{HC}(\tau) e^{\int_0^\tau g(s) ds} d\tau \right] \geq 0,$$

where $g(t) = -\beta_H S_H(t) + \gamma_H + \mu_H + d$.

Similarly, $R_H, R_C, R_{HC} \geq 0$ can be shown using (2) and the fact that $I_H, I_C, I_{HC} \geq 0$. □

3.2. **Boundedness of the total population.**

Theorem 2. *The total population remains bounded for all time t.*

Proof. Let N denote the total population. Then:

$$N(t) = S_H(t) + S_C(t) + S_{HC}(t) + I_H(t) + I_C(t) + I_{HC}(t) + R_H(t) + R_C(t) + R_{HC}(t).$$

Differentiating $N(t)$ gives:

$$N'(t) = \Lambda - dN(t) - \mu_H I_H - \mu_C I_C - (\mu_H + \mu_C) I_{HC},$$

where $\Lambda = \Lambda_H + \Lambda_C + \Lambda_{HC}$.

This implies:

$$N'(t) \leq \Lambda - dN(t),$$

whose solution is:

$$N(t) \leq e^{-dt} \left[N(0) + \Lambda \int_0^t e^{ds} ds \right].$$

Thus:

$$N(t) \leq e^{-dt} \left[N(0) - \frac{\Lambda}{d} \right] + \frac{\Lambda}{d}.$$

Therefore:

$$\begin{cases} N(t) \leq \frac{\Lambda}{d} & \text{if } N(0) \leq \frac{\Lambda}{d}, \\ N(t) \leq N(0) & \text{if } N(0) \geq \frac{\Lambda}{d}. \end{cases} \tag{3}$$

Hence:

$$0 \leq N(t) \leq \max(N(0), \frac{\Lambda}{d}).$$

Consequently:

$$\Omega_0 = \left\{ X = (S_H, S_C, S_{HC}, I_H, I_C, I_{HC}, R_H, R_C, R_{HC}) \in \mathbb{R}^9 \mid 0 \leq N(t) \leq \max(N(0), \frac{\Lambda}{d}) \right\}. \tag{4}$$

□

3.3. **Equilibrium Points without Disease (DFE).** We solve the system when there are no diseases in the population, i.e., when $I_H = I_C = I_{HC} = 0$. Thus, we have

$$E_0 = \left(\frac{\Lambda_H}{d}, \frac{\Lambda_C}{d}, \frac{\Lambda_{HC}}{d}, 0, 0, 0, 0, 0, 0 \right)$$

which is the unique equilibrium point without disease (DFE).

3.4. **Basic Reproduction Number.** Let $\mathcal{F} = (\beta_H S_H I_H + \alpha_H S_H I_{HC}, \beta_C S_C I_C + \alpha_C S_C I_{HC}, \beta_{HC} S_H I_{HC})^T$ represent the new infections in the infected classes I_H, I_C, I_{HC} and $\mathcal{V}$ represent other flows within and outside the infected classes I_H, I_C, I_{HC} (note that $\mathcal{V}$ has a negative sign).

The basic reproduction number is the average number of secondary infections produced by an infected individual when introduced into a population of susceptibles. In our case, $\mathcal{V}$ is given by:

$$\mathcal{V} = \begin{pmatrix} (\gamma_H + d_H + \mu_H) I_H \\ (\gamma_C + d_C + \mu_C) I_C \\ (\gamma_H + \gamma_C + \mu_H + \mu_C + d) I_{HC} \end{pmatrix}$$

The matrix of new infections F and the transfer matrix between compartments V are the Jacobian matrices obtained by differentiating $\mathcal{F}$ and $\mathcal{V}$ with respect to the infected variables, i.e.:

$$\mathbf{D}\mathcal{F}(E_0) = \left. \frac{\partial \mathcal{F}}{\partial (I_H, I_C, I_{HC})} \right|_{E_0} \tag{5}$$

Thus, we have:

$$F = \begin{pmatrix} \frac{\beta_H \Lambda_H}{d} & 0 & \frac{\alpha_H \Lambda_H}{d} \\ 0 & \frac{\beta_C \Lambda_C}{d} & \frac{\alpha_C \Lambda_C}{d} \\ 0 & 0 & \frac{\beta_{HC} \Lambda_{HC}}{d} \end{pmatrix} \tag{6}$$

and

$$V = \begin{pmatrix} \gamma_H + \mu_H + d & 0 & 0 \\ 0 & \gamma_C + \mu_C + d & 0 \\ 0 & 0 & \gamma_H + \gamma_C + \mu_H + \mu_C + d \end{pmatrix}.$$

Thus, the matrix of the next generation is given by:

$$FV^{-1} = \begin{pmatrix} \frac{\beta_H \Lambda_H}{d} & 0 & \frac{\alpha_H \Lambda_H}{d} \\ 0 & \frac{\beta_C \Lambda_C}{d} & \frac{\alpha_C \Lambda_C}{d} \\ 0 & 0 & \frac{\beta_{HC} \Lambda_{HC}}{d} \end{pmatrix} \begin{pmatrix} \frac{1}{\gamma_H + \mu_H + d} & 0 & 0 \\ 0 & \frac{1}{\gamma_C + \mu_C + d} & 0 \\ 0 & 0 & \frac{1}{\gamma_H + \gamma_C + \mu_H + \mu_C + d} \end{pmatrix}$$

i.e.

$$FV^{-1} = \begin{pmatrix} \frac{\beta_H \Lambda_H}{d(\gamma_H + \mu_H + d)} & 0 & 0 \\ 0 & \frac{\beta_C \Lambda_C}{d(\gamma_C + \mu_C + d)} & 0 \\ 0 & 0 & \frac{\beta_{HC} \Lambda_{HC}}{d(\gamma_H + \gamma_C + \mu_H + \mu_C + d)} \end{pmatrix}$$

Since FV^{-1} is diagonal, its eigenvalues are the diagonal elements:

$$\lambda_1 = \frac{\beta_H \Lambda_H}{d(\gamma_H + \mu_H + d)}, \quad \lambda_2 = \frac{\beta_C \Lambda_C}{d(\gamma_C + \mu_C + d)}, \quad \lambda_3 = \frac{\beta_{HC} \Lambda_{HC}}{d(\gamma_H + \gamma_C + \mu_H + \mu_C + d)}.$$

Thus,

$$\mathcal{R}_0 = \rho(FV^{-1}) = \max(\mathcal{R}_1, \mathcal{R}_2, \mathcal{R}_3) \tag{7}$$

where

$$\mathcal{R}_1 = \frac{\beta_H \Lambda_H}{d(\gamma_H + \mu_H + d)}, \quad \mathcal{R}_2 = \frac{\beta_C \Lambda_C}{d(\gamma_C + \mu_C + d)}, \quad \mathcal{R}_3 = \frac{\beta_{HC} \Lambda_{HC}}{d(\gamma_H + \gamma_C + \mu_H + \mu_C + d)}.$$

3.5. **Local stability analysis.**

Theorem 3. *The DFE E_0 is locally asymptotically stable if $\mathcal{R}_0 < 1$.*

Proof. The Jacobian matrix at the point E_0 is

$$J(E_0) = \begin{pmatrix} -d & 0 & 0 & -\frac{\beta_H \Lambda_H}{d} & 0 & -\frac{\alpha_H \Lambda_H}{d} & 0 & 0 & 0 \\ 0 & -d & 0 & 0 & -\frac{\beta_C \Lambda_C}{d} & -\frac{\alpha_C \Lambda_C}{d} & 0 & 0 & 0 \\ 0 & 0 & -d & 0 & 0 & -\frac{\beta_{HC} \Lambda_{HC}}{d} & 0 & 0 & 0 \\ 0 & 0 & 0 & \frac{\beta_H \Lambda_H}{d} - \gamma_H - \mu_H - d & 0 & \frac{\alpha_H \Lambda_H}{d} & 0 & 0 & 0 \\ 0 & 0 & 0 & 0 & \frac{\beta_C \Lambda_C}{d} - \gamma_C - \mu_C - d & \frac{\alpha_C \Lambda_C}{d} & 0 & 0 & 0 \\ 0 & 0 & 0 & 0 & 0 & \frac{\beta_{HC} \Lambda_{HC}}{d} - \gamma_H - \gamma_C - \mu_H - \mu_C - d & 0 & 0 & 0 \\ 0 & 0 & 0 & \gamma_H & 0 & 0 & -d & 0 & 0 \\ 0 & 0 & 0 & 0 & \gamma_C & 0 & 0 & -d & 0 \\ 0 & 0 & 0 & 0 & 0 & \gamma_H + \gamma_C & 0 & 0 & -d \end{pmatrix} \tag{8}$$

The eigenvalues of this matrix are $\lambda_1 = \lambda_2 = \lambda_3 = \lambda_4 = \lambda_5 = \lambda_6 = -d$, $\lambda_7 = \frac{\beta_H \Lambda_H}{d} - \gamma_H - \mu_H - d$, $\lambda_8 = \frac{\beta_C \Lambda_C}{d} - \gamma_C - \mu_C - d$, and $\lambda_9 = \frac{\beta_{HC} \Lambda_{HC}}{d} - \gamma_H - \gamma_C - \mu_H - \mu_C - d$.

Thus,

$$\lambda_7 = (\gamma_H + \mu_H + d)(\mathcal{R}_1 - 1) \tag{9}$$

$$\lambda_8 = (\gamma_C + \mu_C + d)(\mathcal{R}_2 - 1) \tag{10}$$

$$\lambda_9 = (\gamma_H + \gamma_C + \mu_H + \mu_C + d)(\mathcal{R}_3 - 1) \tag{11}$$

If $\mathcal{R}_0 < 1$, then all the eigenvalues are negative.

Thus, the equilibrium point E_0 is locally asymptotically stable when $\mathcal{R}_0 < 1$. □

3.6. **Global stability of the disease-free equilibrium point.**

Theorem 4. *The DFE E_0 is globally asymptotically stable if $\mathcal{R}_0 < 1$.*

Proof. Let's check the conditions of the Castillo-Chavez theorem.

(1) Let $z_1 = (S_H, S_C, S_{HC}, R_H, R_C, R_{HC})$ represent the class of uninfected individuals, and $z_2 = (I_H, I_C, I_{HC})$ represent the class of infected individuals. For $z_2 = 0$, the system (1) becomes

$$\frac{dS_H}{dt} = \Lambda_H - dS_H \tag{12}$$

$$\frac{dS_C}{dt} = \Lambda_C - dS_C \tag{13}$$

$$\frac{dS_{HC}}{dt} = \Lambda_{HC} - dS_{HC} \tag{14}$$

$$\frac{dR_H}{dt} = -dR_H \tag{15}$$

$$\frac{dR_C}{dt} = -dR_C \tag{16}$$

$$\frac{dR_{HC}}{dt} = -dR_{HC} \tag{17}$$

Solving each of these equations, we get

$$S_H(t) = e^{-dt}\left[S_H(0) - \frac{\Lambda_H}{d}\right] + \frac{\Lambda_H}{d}$$

$$S_C(t) = e^{-dt}\left[S_C(0) - \frac{\Lambda_C}{d}\right] + \frac{\Lambda_C}{d}$$

$$S_{HC}(t) = e^{-dt}\left[S_{HC}(0) - \frac{\Lambda_{HC}}{d}\right] + \frac{\Lambda_{HC}}{d}$$

and $R_H(t) = R_C(t) = R_{HC}(t) = ke^{-dt}$. Taking the limit as $t \to \infty$, we get

$$\lim_{t \to \infty} z_1 = \left(\frac{\Lambda_H}{d}, \frac{\Lambda_C}{d}, \frac{\Lambda_{HC}}{d}, 0, 0, 0\right) = z_1^\star$$

Hence, $z_1^\star$ is globally stable when $z_2 = 0$.

(2) Now consider the system of the infected individuals:

$$\frac{dI_H}{dt} = \beta_H S_H I_H - \gamma_H I_H + \alpha_H S_H I_{HC} - (d + \mu_H) I_H = g_1 \tag{18}$$

$$\frac{dI_C}{dt} = \beta_C S_C I_C - \gamma_C I_C + \alpha_C S_C I_{HC} - (d + \mu_C) I_C = g_2 \tag{19}$$

$$\frac{dI_{HC}}{dt} = \beta_{HC} S_{HC} I_{HC} - (\gamma_H + \gamma_C) I_{HC} - (d + \mu_{HC}) I_{HC} = g_3 \tag{20}$$

Let $A = \frac{\partial(g_1, g_2, g_3)}{\partial z_2}(E_0)$. We have

$$A = \begin{pmatrix} \beta_H \frac{\Lambda_H}{d} - \gamma_H - \mu_H - d & 0 & \alpha_H \frac{\Lambda_H}{d} \\ 0 & \beta_C \frac{\Lambda_C}{d} - \gamma_C - \mu_C - d & \alpha_C \frac{\Lambda_C}{d} \\ 0 & 0 & \beta_{HC} \frac{\Lambda_{HC}}{d} - \gamma_H - \gamma_C - \mu_H - \mu_C - d \end{pmatrix}$$

Since

$$\hat{G} = Az_2 - \begin{pmatrix} g_1 \\ g_2 \\ g_3 \end{pmatrix}$$

we have

$$\hat{G} = \begin{pmatrix} \left(\frac{\Lambda_H}{d} - S_H\right)(\beta_H I_H + \alpha_H I_{HC}) \\ \left(\frac{\Lambda_C}{d} - S_C\right)(\beta_C I_C + \alpha_C I_{HC}) \\ \beta_{HC} I_{HC} \left(\frac{\Lambda_{HC}}{d} - S_{HC}\right) \end{pmatrix} \geq 0$$

in the domain

$$\Omega_1 = \left\{ (S_H, S_C, S_{HC}) \in \mathbb{R}^3 \mid 0 \leq S_H \leq \frac{\Lambda_H}{d}; 0 \leq S_C \leq \frac{\Lambda_C}{d}; 0 \leq S_{HC} \leq \frac{\Lambda_{HC}}{d} \right\}$$

Hence, E_0 is globally asymptotically stable when $\mathcal{R}_0 < 1$. □

4. Sensitivity analysis

We will use the data in (3) for the numerical sensitivity analysis. It should be noted that some data were not found in the literature regarding co-infection, and we have assumed them. However, the recruitments are random.

Parameters	Intervals	Values	References
Λ_H	-	10	assumed
Λ_C, Λ_{HC}	-	5	assumed
β_H	0.000004-0.15	0.000012	[3]
β_C	0.000001-0.1	0.000032	[12]
β_{HC}	0.000002-0.015	0.00022	assumed
μ_H	0.0001-0.001	0.0007	[3]
μ_C	0.0001-0.001	0.0006	[14]
γ_H	0.004-0.15	0.02	[3]
γ_C	0.004-0.15	0.02	[14]
α_H	0.0004-0.1	0.00115	assumed
α_C	0.00002-0.1	0.00125	assumed
d	0.00001-0.1	0.0001	[14]

Table 3. Model parameters table.

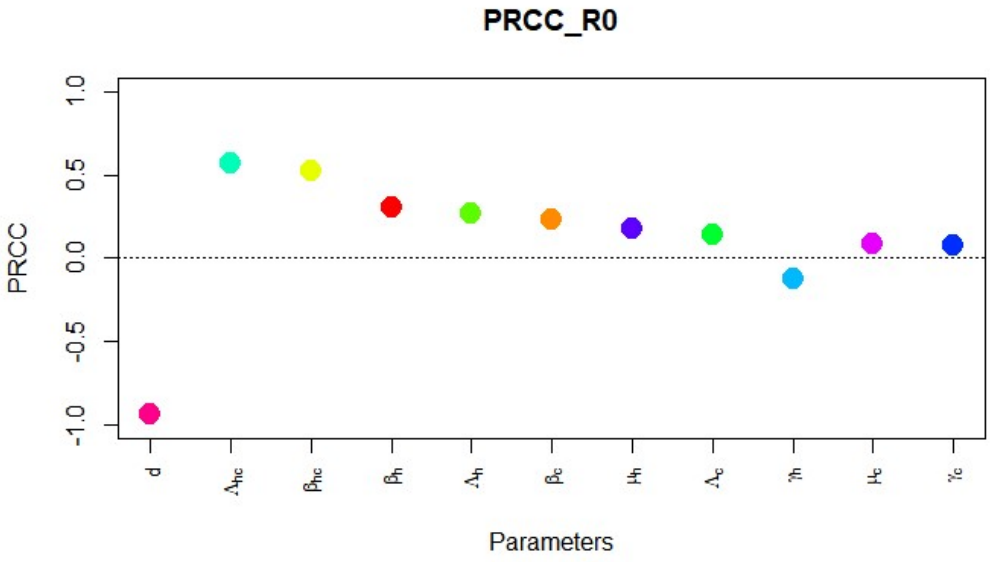

FIGURE 2. PRCC of $\mathcal{R}_0$ using the parameter values in (3).

Interpretation: Figure (2) indicates that parameters far from the origin influence the variation of $\mathcal{R}_1$, $\mathcal{R}_2$, and $\mathcal{R}_3$. For example, β_H, β_C, β_{HC}, and the recruitments. However, this PRCC suggests promoting natural death, which we cannot consider. Therefore, to control $\mathcal{R}_0$, these parameters must be controlled.

5. Numerical simulations

We use the parameter data from Table (3) for numerical simulations to graphically illustrate the results. First, we will simulate with the exact data, then we will adjust some parameters recommended by the PRCC to see the trend of the curves.

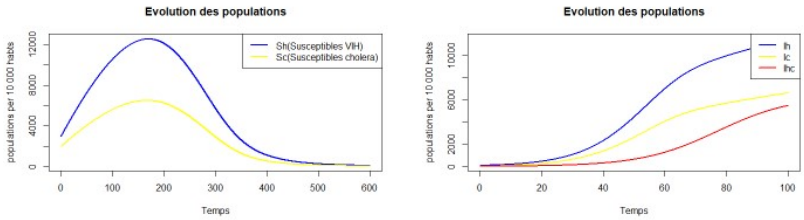

(a) Susceptible populations (b) Infected populations

FIGURE 3. Temporal behavior of the susceptible and infected populations (with $\mathcal{R}_1 = 48.5$, $\mathcal{R}_2 = 42.35$, $\mathcal{R}_3 = 38.1$, and $\beta_H = 0.00022$, $\beta_H = 0.00012$, and $\beta_{HC} = 0.00034$).

Interpretation: Figures (3(a))-(3(b)) show that the susceptible population will disappear within the next 400 days due to the high reproduction rate of the infection. This phenomenon is further strengthened by a high contact rate between susceptible and infected individuals, promoting rapid disease transmission.

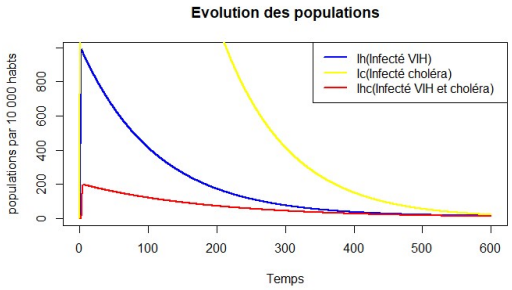

FIGURE 4. Temporal behavior of infected populations (with $\mathcal{R}_1 = 1.05$, $\mathcal{R}_2 = 0.95$, $\mathcal{R}_3 = 0.81$, and $\beta_H = 0.0000022$, $\beta_C = 0.0000012$, and $\beta_{HC} = 0.0000034$).

Interpretation: Figure (4) indicates that, when the contact rate between susceptible and infected individuals is significantly reduced, the infected population will disappear after the next 400 days for cholera and 500 days for HIV, because biologically speaking, the recovery from cholera is faster than that from HIV.

6. Conclusion

The studied HIV-Cholera co-infection model is of the SIR type. We have established the local and global stability of the disease-free equilibrium (DFE). We also performed a sensitivity analysis of the reproduction number. This study allowed us to understand that the most influential parameters for controlling the disease would be the contact rates β_H, β_C, and β_{HC}. Numerical results show that both diseases will disappear when the basic reproduction number $\mathcal{R}_0$ remains below one.

As future work, we plan to explore the endemic equilibrium points and investigate whether there will be any bifurcation.

References

[1] Agarwal M., Verma V. Modeling and analysis of the spread of an infectious disease cholera with environmental fluctuations. *Applications and Applied Mathematics: An International Journal (AAM)*, 7(1): 27, 2012.

[2] Al-Arydah M., Mwasa A., Tchuenche J. M., Smith R. J. Modeling cholera disease with education and chlorination. *Journal of Biological Systems*, 21(4): 1340007, 2013.

[3] Alassane M. Modélisation et simulations numériques de l'épidémie du VIH-SIDA au Mali. *PhD Thesis, INSA de Lyon ; Université du Mali*, 2012. Disponible : `https://theses.hal.science/tel-01339825`.

[4] AFRIQUE SUBSAHARIENNE, *UN COUPLE MAUDIT*. Article de synthèse, 2010.

[5] Bessimbaye N., Moussa A. M., Mbanga D., Tidjani A., Mahamat, S. O., Ngawara, M. N., Ngarnayal, G., Fissou, H. Y., Sangare, L., Ndoutamia, G., & al. Séroprévalence de l'Ag HBs et de l'anticorps Anti VHC chez les personnes infectées par le VIH1 à N'Djamena, Tchad. *Bulletin de la Société de pathologie exotique*, 107, 327-331, 2014.

[6] Colwell R. R. Climat mondial et maladies infectieuses: le paradigme du choléra. *Science*, 274(5295): 2025–2031, 1996.

[7] Codeço C. T. Endemic and epidemic dynamics of cholera: the role of the aquatic reservoir. *BMC Infectious Diseases*, 1: 1–14, 2001.

[8] Eliot E., Daudé E., Bonnet E. Interpréter les épidémies du passé: l'exemple de l'épidémie du choléra-morbus en Normandie en 1832.

[9] Griffith D. C., Kelly-Hope L. A., Miller M. A. Review of reported cholera epidemics worldwide, 1995-2005. *The American Journal of Tropical Medicine and Hygiene*, 75(5): 973–977, 2006.

[10] Longini Jr I. M., Nizam A., Ali M., Yunus M., Shenvi N., Clemens J. D. Controlling endemic cholera with oral vaccines. *PLoS Medicine*, 4(11): e336, 2007.

[11] Ozanne, Alexandra. *Activation immunitaire, immuno-sénescence et inflammation : Analyses statistiques des liens avec les comorbidités non liées au VIH lors de l'infection par le VIH.* Thèse de doctorat, Université de Bordeaux, 2017. Disponible en ligne : `https://theses.hal.science/tel-01757534`.

[12] Pasteur Institute. *Cholera: Symptoms, treatment, prevention*; 2024. Available at: `https://www.pasteur.fr/en/medical-center/disease-sheets/cholera`. Accessed December 6, 2024.

[13] C. Régional de l'Afrique. *Lignes directrices consolidées sur l'utilisation des médicaments antirétroviraux pour le traitement et la prévention des infections à VIH; recommandations pour une approche de sante publique–implications pour la Région africaine: rapport du Secrétariat*, 2013.

[14] Tien J. H., Earn D. J. D. Multiple transmission pathways and disease dynamics in a waterborne pathogen model. *Bulletin of Mathematical Biology*, 72: 1506–1533, 2010.

[15] TO, CH., ND, M., ANG, NG., DJ, N., & RI, V. Etude de la séroprévalence du VIH chez les patients atteints d'une tuberculose pulmonaire en 1999 au Tchad. *Médecine tropicale*, 62(6): 627, 2002.

Abdramane Annour Saad
Laboratory of Mathematical Modeling, Computer Science, Applications and Simulations (L2MIAS), University of N'Djamena, N'Djamena, Chad
Email address: `annoursaadabdramane31@gmail.com, saad@abdramane.com`

Djimramadji Hippolyte
Laboratory L2MIAS, University of N'Djamena, N'Djamena, Chad
Email address: `hippolytedjimramadji@gmail.com`

Mahamat Saleh Daoussa Haggar
Laboratory L2MIAS, University of N'Djamena, N'Djamena, Chad
Email address: `msdhaggar@gmail.com`